STRENGTH, RELIABILITY AND ASSET MANAGEMENT OF CORRODING RC STRUCTURES

Mark G. Stewart[1]

[1]**The University of Newcastle, NSW, Australia**

SUMMARY: Many reinforced concrete (RC) structures are deteriorating due to chloride and/or carbonation induced corrosion. A spatial time-dependent structural reliability model is developed that calculates (i) strength degradation with time, (ii) probability and extent of corrosion damage (cover cracking) and (iii) probability of collapse for RC structures subject to pitting corrosion. This enables accurate service life predictions to be made. These models include the spatial and temporal variability of cover, concrete strength, chloride exposure, corrosion rate, corrosion initiation, cover cracking, pit depth, etc., as well as the time-dependent variability of loadings. The effect of maintenance strategies, such as periodic inspections, on updated reliability and service life predictions are also estimated. Illustrative examples are given for RC beams whose performance and reliability are updated using visual inspection findings of corrosion damage. Information about service life prediction, and updating based on (new) condition assessment findings, is essential for asset management of deteriorating structures.

Keywords: Concrete, Structural Reliability, Corrosion, Service Life Prediction.

1. INTRODUCTION

Many reinforced concrete (RC) structures are deteriorating due to chloride and/or carbonation induced corrosion. Reinforcement corrosion causes metal loss and voluminous corrosion products, eventually resulting in longitudinal cracking and spalling of concrete cover, leading to loss of structural capacity. Chloride-initiated reinforcement corrosion causes pitting corrosion which causes a spatially distributed reduction of the cross-sectional area of reinforcement. This chloride-induced deterioration process is influenced by concrete strength, concrete cover, surface chloride concentration and other material, environmental and dimensional properties which vary spatially and temporally over the structure. For example, Fazio et al (1999) measured corrosion parameters and concrete properties of a 39 year old Canadian bridge deck and found significant spatial variability in chloride content, concrete cover, concrete strength and corrosion damage. The corrosion rate was found to differ by up to two orders of magnitude across the bridge deck, and concrete cover varied from less than 25 mm to over 50 mm.

A spatial time-dependent reliability analysis is a useful technique for quantifying risk and uncertainty for spatial and temporal degradation processes (e.g., Stewart 2004, Li et al 2004, Stewart and Mullard 2007). Obviously, there is a strong relationship between reinforcement corrosion loss and corrosion-induced concrete cover cracking, although there remains significant uncertainty as to the precise quantitative nature of the relationship. Thus, corrosion damage of the concrete cover (cover cracking) may be treated as an indicator of corrosion loss which then affects structural resistance, structural safety and reliability. A spatial time-dependent structural reliability model is developed herein that calculates (i) strength degradation with time, (ii) probability and extent of corrosion damage (cover cracking) and (iii) probability of collapse for RC structures subject to pitting corrosion. A random field model is used to simulate the material, environmental and dimensional spatial variability of the RC beam which allows for inspection results (corrosion damage) to quantitatively assess the condition of the structure (pitting corrosion) and incorporating this information into structural safety and reliability prediction. The term ‘corrosion damage’ herein refers to corrosion-induced surface cracking widths exceeding 1 mm, which would be classified as severe cover cracking readily observable by visual inspection. This enables accurate service life predictions to be made. These models include the spatial and temporal variability of cover, concrete strength,

chloride exposure, corrosion rate, corrosion initiation, cover cracking, pit depth, etc., as well as the time-dependent variability of loadings. The effect of maintenance strategies, such as periodic visual inspections, on updated reliability and service life predictions are also estimated. Illustrative examples are given for RC beams whose performance and reliability are updated using visual inspection findings of corrosion damage. Information about service life prediction, and updating based on (new) inspection findings, is essential for asset management of deteriorating structures.

2. CORROSION-INDUCED DETERIORATION PROCESS

The performance and degradation process of RC structures subject to chloride attack can be divided into two limit (failure) states: (i) severe cracking of concrete cover (corrosion damage) and (ii) structural collapse caused by pitting (highly localised) corrosion. Predictive models for the deterioration process to be used in the present paper are described in detail elsewhere (Vu and Stewart 2000, Vu et al 2005, Stewart and Mullard 2007, Stewart 2009), but will be briefly reviewed herein. Note that many other deterioration models have been developed for RC behaviour, which if deemed more appropriate, can readily be incorporated into the stochastic and reliability framework developed in the present paper.

2.1 Corrosion Damage to Concrete Cover

Corrosion-induced cover cracking occurs on the concrete surface above and parallel to the rebars. The various stages of crack growth can be described in three stages:

(i) Corrosion initiation (T_i);

(ii) Crack initiation (t_{1st}, time to first cracking - hairline crack of 0.05 mm width), and;

(iii) Crack propagation (T_{ser}, time for crack to develop from crack initiation to a limit crack width, w).

Much research has focused on developing robust predictive models for time to corrosion initiation, time to crack initiation and time to severe cracking – many models have been developed - see Val and Stewart (2009) for a detailed literature review of existing models.

Corrosion will initiate when the chloride content around the reinforcement exceeds a threshold value. Fick's second law is used to describe the chloride penetration into concrete and calculate the time to corrosion initiation T_i. In this case, the surface chloride content C_o, apparent diffusion coefficient D, and threshold chloride concentration C_{cr} are needed. A model developed by Papadakis et al (1996) is used to consider the influence of mix proportions on diffusion coefficient. This model requires w/c (water-cement) ratio as an input parameter, which is estimated from concrete compressive strength using Bolomey's formula.

To predict the development of corrosion-induced deterioration with time the rate of corrosion needs to be known – this is usually described in terms of the corrosion current density, i_{corr}. Vu and Stewart (2000) propose that for RH≥80% the corrosion current density in the first year after corrosion initiation can be expressed empirically as

$$i_{corr}(1) = \frac{27.0(1-w/c)^{-1.64}}{C} \quad (\mu A/cm^2) \qquad (1)$$

where $i_{corr}(1)$ is the corrosion rate at the start of corrosion propagation, w/c is the water-cement ratio and cover C is given in mm. In general, the corrosion rate can then be expressed as a time-dependent variable as formation of rust products impedes the access of reactive products to the steel surface resulting in reduced corrosion rates with time; hence,

$$i_{corr}(t) = i_{corr}(1) \times \alpha (t - T_i)^{\beta} \qquad (t - T_i) > 1 \text{ year} \qquad (2)$$

where α and β are constants equal to 0.85 and -0.3, respectively.

As there is a porous zone around the steel reinforcing bar the corrosion products must firstly fill this porous zone before the products start to induce internal pressure on the surrounding concrete. Therefore, some of corrosion products do not contribute to the expansive pressure on the concrete. This approach to crack initiation has been used by El Maaddawy and Soudki (2007) and their model is used herein. The thickness of the porous zone (δ_0) is typically in the range of 10 - 20 μm. It should be noted, that the accuracy of the time to severe cracking is dominated by the accuracy of time to corrosion initiation (T_i) and the time since crack initiation to reach a limit crack width (t_{ser}), and so service life predictions are relatively insensitive to the crack initiation model (Stewart and Mullard 2007).

The time (after corrosion initiation) for cracking of the concrete surface to reach a crack width of w mm is:

$$t_{sp} = t_{1st} + t_{ser} \approx t_{1st} + k_R \frac{0.0114}{i_{corr}} \left[A \left(\frac{C}{w/c} \right)^B \right] \quad 0.3 \text{ mm} \le w \le 1.0 \text{ mm} \qquad (3)$$

where

$$k_R \approx 0.95 \left[\exp\left(-\frac{0.3 i_{corr(exp)}}{i_{corr}} \right) - \frac{i_{corr(exp)}}{2500 i_{corr}} + 0.3 \right] \qquad (4)$$

and where t_{1st} is the time to crack initiation, t_{ser} is the time since crack initiation to reach a limit crack width (years), i_{corr} is the corrosion current density ($\mu A/cm^2$) assumed constant with time, A and B are empirical constants and k_R is a rate of loading correction factor where $i_{corr(exp)}$ is the accelerated corrosion rate used to derive constants A and B. In the present case $i_{corr(exp)}$=100 $\mu A/cm^2$ and A=700 and B=0.23 for w=1.0 mm. The model was developed from test for 16 mm diameter reinforcement. Times to severe cracking as assumed to be 25% lower for 27 mm diameter reinforcement (Stewart and Suo 2009). The time from corrosion initiation to crack initiation (t_{1st}) is calculated by the method proposed by El Maaddawy and Soudki (2007).

Note the Vu et al (2005) model failed to consider the effect of bar diameter and confinement of reinforcement. Hence, an improved corrosion-induced cover cracking model has recently been developed by Mullard and Stewart (2009):

$$t_{sp} = t_{1st} + t_{ser} = t_{1st} + k_R \frac{w - 0.05}{k_c r_{crack}} \left(\frac{0.0114}{i_{corr}} \right) \quad 0.1 \le \psi_{cp} \le 1, \ 0.25 \le k_R \le 1, \ k_c \ge 1.0, \ w \le 1.0 \text{ mm} \qquad (5)$$

$$\psi_{cp} = \frac{C}{D f'_t} \qquad r_{crack} = 0.0008 e^{-1.7 \psi_{cp}} \quad 0.1 \le \psi_{cp} \le 1.0 \qquad (6)$$

where ψ_{cp} is the cover cracking parameter, r_{crack} is the rate of crack propagation in mm/hr, w is the crack width (mm), C is concrete cover in mm, D is reinforcing bar diameter in mm, f'_t is the concrete tensile strength in MPa, and k_c is the confinement factor that represents an increase in crack propagation due to the lack of concrete confinement around external reinforcing bars. If the reinforcing bar is in an internal location then k_c=1, but for rebars located at edges and corners of RC structures then k_c is in the range of 1.2 to 1.4. Although the data is limited, there appears to be a trend where k_c increases as ψ_{cp} increases. A statistical analysis of model accuracy to account for variabilities between model prediction and experimental data is essential for stochastic or reliability analyses where statistics for model error are required. Hence, the statistics for model error for r_{crack} (ME_{rcrack}) are: mean(ME_{rcrack}) = 1.04 and COV(ME_{rcrack}) = 0.09 (COV = coefficient of variation). For more details of the improved cover cracking model see Mullard and Stewart (2009).

If the corrosion rate is modelled as time variant by Eqn. (2) then time to severe cracking will be longer than that predicted by Eqns. (3-6). Hence, if the amount of corrosion products to produce cracking is the same for both time variant and time invariant corrosion rates, then Vu et al. (2005) propose that the time to excessive cracking for a time variant corrosion rate T_{sp} is

$$T_{sp} = \left[\frac{\beta + 1}{\alpha} \times \left(t_{sp} - 1 + \frac{\alpha}{\beta + 1} \right) \right]^{1/\beta + 1} \qquad \textbf{t}_{\textbf{sp}} \textbf{ > 1 year and } \textbf{w}_{\textbf{lim}} \textbf{ ≤ 1 mm} \qquad \textbf{(7)}$$

2.2 Pitting Corrosion

Two concrete test specimens were subject to accelerated corrosion tests to simulate pitting corrosion attack on reinforcement in a chloride-concrete environment. Each specimen was a RC rectangular slab with dimensions 550 × 1000 × 250 mm thickness. The top mat of the slab contained four reinforcing bars with 10-20 mm cover. Two bar diameters were used: Y16-16 mm and Y27-27 mm. The steel reinforcing bars used for this study were round mild steel bars. The concrete was ready-mix commercially supplied with mix design typical of that used in Australia. The aggregates used were 7 to 20 mm coarse gravel aggregates and the fine aggregates were composed of coarse sand and dune sand. The concrete mix contained 210 kg/m^3 of Ordinary Portland (Type I) cement, 55 kg/m^3 of fly ash, and 710 kg/m^3 and 800 kg/m^3 of fine and course aggregates, respectively. Three percent of $CaCl_2$ by weight of cement was added to the concrete mix to induce corrosion. Specimens were moist-cured for 28 days before testing. The average 28-day compressive strength was f'_{cyl}=23.4 MPa.

The accelerated corrosion process was introduced to the steel using an impressed electric current of 100 μA/cm2. This experimental set-up is widely used for accelerated corrosion tests for predicting pit depths, cover cracking and loss of reinforcing bar strength for RC components. At the completion of each corrosion test the specimen was broken up and the steel then cleaned, dried and weighed using the method as specified by ASTM G1-03 to calculate the actual corrosion rate. The average corrosion loss was 10%. The pit-depth in the corroded steel was then measured using a micrometer gauge, which has an accuracy of 0.01 mm.

Maximum pit-depths were measured for each 100 mm length of the reinforcing bar for each of the four reinforcing bars, each bar divided into eight equal 100 mm lengths. The pit density varied greatly, with some 100 mm lengths containing a single pit, and others up to six pits at different locations along the sample length. In each case, only the maximum pit-depth for each 100 mm length was used for statistical analysis. Pit depths were not measured within 100 mm of the end of a bar to avoid 'edge affects'. The maximum pit depth will normally exceed the penetration based on general (uniform) corrosion ($P_{av}=0.0116i_{corr}t$). A pitting factor $R=p/P_{av}$ is then used to define the extent of corrosion pitting where p is the maximum pit depth. Statistics for pitting factors for Y16 and Y27 bars are shown in Table 1, for a sample size of 32.

Table 1. Statistics of Pitting Corrosion Obtained from Accelerated Corrosion Tests (Stewart and Al-Harthy 2008).

Specimen	i_{corr} ($\mu A/cm^2$)	L (mm)	Diameter (mm)	Time (days)	No. of Samples	Pitting Factor R		Gumbel Parameters	
						mean	COV	μ_o	α_o
Specimen-1	160-185	100	16	78	32	6.2	0.18	5.56	1.16
Specimen-2	125-150	100	27	78	32	7.1	0.17	6.55	1.07

Whilst the top covers were similar, cover cracking occurred at different times which may affect pit propagation. It has also been observed that the pitting factor may reduce with time because as the size of the pit (anode) increases the ratio of anodic area to cathodic will reduce hence reducing the rate of depletion of the pit. Hence, the statistics of pit depths proposed herein should be used with caution.

It was found that R is statistically independent for 100 mm lengths and that a Gumbel (EV-Type I) distribution is the best fit for modelling maximum pit depths for reinforcing bars (Stewart and Al-Harthy 2008). To predict the distribution of maximum pitting factor for a reinforcing bar of length (L_U), the Gumbel statistical parameters can be modified as:

$$\mu = \mu_o + \frac{1}{\alpha_o}\ln\left(\frac{L_U}{L_o}\right) \qquad \alpha = \alpha_o \qquad (8)$$

where the Gumbel parameters μ_o and α_o are derived from statistical analysis of pitting data for reinforcement of length L_o. Note that R is assumed time-invariant, the distribution is truncated at R=1 and Eqn. (8) assumes statistical independence between adjacent reinforcement lengths L_o. The assumption of statistical independence might not always be valid as the steel-concrete interface may not be totally independent between adjacent locations on a reinforcing bar, or even between bars. In the present case, however, statistics for the pitting factor were taken from pit depths measured along and between reinforcing bars, and so the Gumbel parameters given in Table 1 should help capture this variability.

The maximum pit depth (mm) along a reinforcing bar of length L_U is

$$p(t) = 0.0116R\int_{T_i}^{t} i_{corr}(t)dt \qquad t > T_i \qquad (9)$$

Reinforcement yield strength (f_y) reduces linearly with corrosion loss (Du et al 2005):

$$f_y(t) = \left(1.0 - \alpha_y Q_{corr}(t)\right) f_{y0} \qquad (10)$$

where f_{y0} is the yield stress of an uncorroded reinforcing bar, α_y is an empirical coefficient (=0.005), and $Q_{corr}(t)$ is the percentage corrosion loss measured as $A_{pit}(t)/A_{stnom}x100\%$ where A_{stnom} is the cross-sectional area of an uncorroded reinforcing bar. The pit configuration is shown in Figure 1. The reinforcing bar is subdivided into m elements of length Δ, see Figure 2. A reinforcing bar will be subject to multiple pits, and the deepest pit (Gumbel distribution described by Eqn.

(8)) is assumed to occur in the middle of each element. Hence the capacity of an element is taken at the cross-section of the middle of the element.

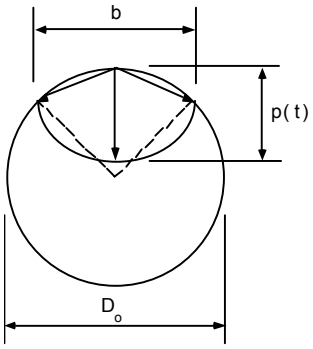

Figure 1 Pit Configuration

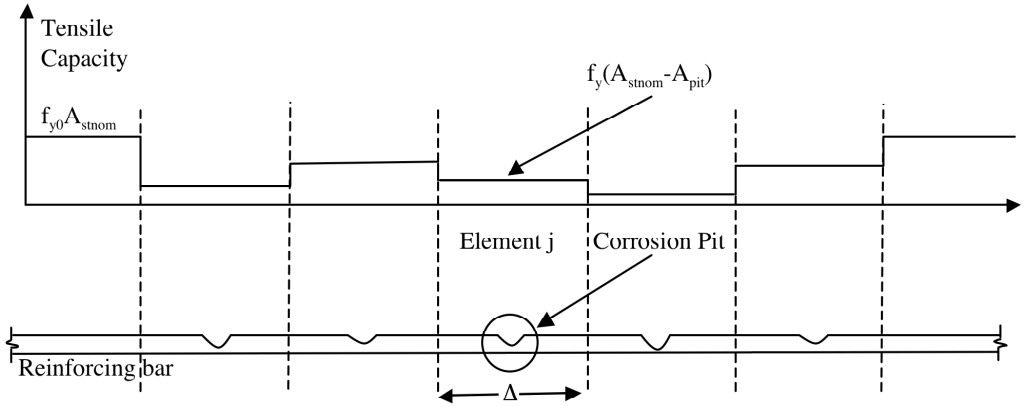

Figure 2 Spatial Capacity of Corroded Reinforcing Bar

There is general consensus that the mechanical behaviour of reinforcing bars changes from ductile to non ductile (brittle) as corrosion loss increases. What is less clear is the level of corrosion loss when the mechanical behaviour transitions from ductile to non ductile behaviour and how this is affected by steel type. Clearly, the progression from ductile to brittle behaviour is spatially and time-dependent. Stewart (2009) found that for a RC structural component that comprises of many reinforcing bars and elements there is a strong likelihood of non-ductile behaviour in at least one corroding reinforcing bar irrespective of structural configuration. Hence, some reinforcement which is more heavily corroded than other reinforcement will exhibit brittle behaviour, and other (less corroded) reinforcement ductile behaviour. This phenomena is very difficult to model either numerically or by stochastic FEA. As such, Stewart (2009) assumed two bounds on structural resistance and reliability, namely, all reinforcement in a RC structural component exhibits: (i) ductile behaviour or (ii) brittle behaviour. As the capacity of a perfectly brittle parallel system is less than that of a perfectly ductile parallel system, it follows that the actual structural reliability of the RC structural component will thus lie somewhere between these structural reliabilities.

For more details of the pitting corrosion model and the calculation of p(t), $A_{pit}(t)$, $f_y(t)$ and structural capacity see Stewart and Al-Harthy (2008) and Stewart (2009).

3. RANDOM FIELD THEORY AND SPATIAL TIME-DEPENDENT RELIABILITY

It is well accepted that many variables influence the corrosion process, such as concrete strength, concrete cover and surface chloride concentration, are not homogeneous across the surface of structure. Stochastic models that do not include random spatial variability cannot adequately describe the damage and performance characteristics of RC structures.

To implement random field theory the structure is divided into m elements of equal size. For ease of computation, the middle point method is applied to the random field. The values of each element are represented by the values of the centroid of each element and this value is assumed to be constant within the element. Elements in a random field are usually spatially correlated, this means that adjacent elements are highly correlated whereas elements that are further apart will exhibit little (if any) correlation. The Gaussian correlation function is used herein to calculate the correlation coefficient between any two elements. For more details about random field theory, see Vanmarcke (1983). For a RC structure in a chloride contaminated environment simulated by a random field model, several important variables, such as the times to corrosion initiation, crack initiation, severe cracking and the resulting loss of rebar cross-section are described by correlated spatial variables.

A 1D random field is suitable for modelling a RC beam. For a RC beam which is divided into m elements of length Δ (see Figure 3), concrete cover, concrete compressive strength and surface chloride concentration are modelled as 1D random field variables. The chloride diffusion coefficient, w/c ratio and corrosion rate are dependent variables on the concrete compressive strength and/or cover and are thus also spatially variable. For pitting corrosion it is assumed that the pitting factor R of a reinforcing bar between elements are statistically independent which is equivalent to a random field with zero correlation between elements. For example, Figure 4 shows a typical Monte-Carlo simulation realisation of the distribution of pitting factor (R) for six Y27 reinforcing bars each with element length Δ=500 mm.

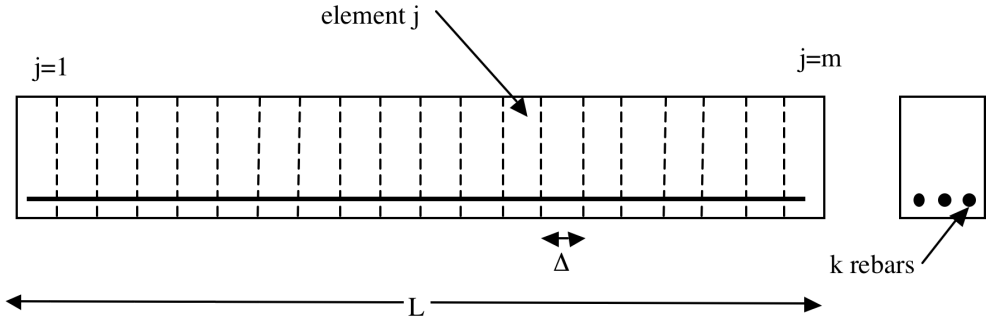

Figure 3 Discretisation of RC Beam

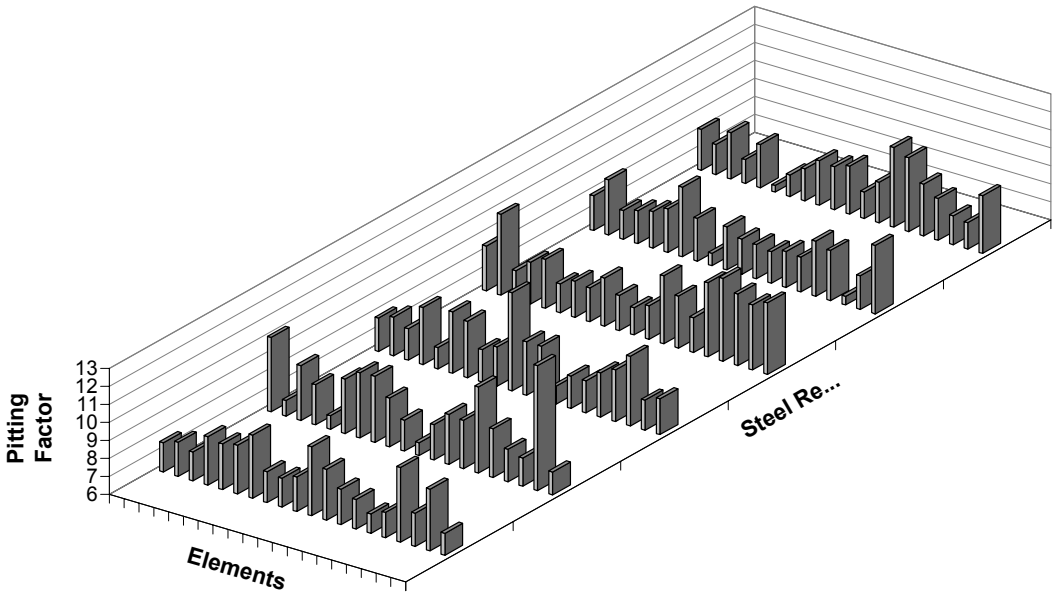

Figure 4 Monte-Carlo Simulation Realisation of Pitting Factors (R) for six Y27 Reinforcing Bars for a 10 m RC Beam Discretised into 20 Elements.

The proportion of a concrete surface with crack widths exceeding the limit width at time t (for a single Monte Carlo simulation realisation) is

$$d_{crack}(t) = \frac{N\left[t > T_{i(j)} + T_{sp(j)}\right]}{m} \times 100\% \qquad (11)$$

where $T_i(j)$ and $T_{sp}(j)$ are the time to corrosion initiation and subsequent time to severe cracking damage of element j (j=1, 2,..., m) respectively, m is the number of elements and N[ ] denotes the number of elements for which $t > T_{i(j)}+T_{sp(j)}$.

For the ultimate strength limit state, a RC beam composing of m elements can be referred to as a series system. As failure of the beam corresponds to failure of the weakest element in the beam, the limit state occurs when load effects $S_j(t)$ exceed resistance $R_j(t)$ at any element at time t

$$G(t) = \min_{j=1,m}\left[R_j(t) - S_j(t)\right] \qquad (12)$$

where $R_j(t)$ is the resistance for element j and $S_j(t)$ is the load effects at the mid-point of element j. For example, the flexural loading capacity of element j of a singly reinforced RC beam is based on layout of k main reinforcing bars which comprise a parallel system. If ductile mechanical behaviour of each reinforcing bar is considered, the time-varying flexural resistance of the j^{th} element of the beam is

$$R_j(t) = ME \sum_{i=1}^{k} A_i(t) f_{yi}(t) \left[d - \frac{\sum_{i=1}^{k} A_i(t) f_{yi}(t)}{1.7 f'_c b} \right] \qquad (13)$$

where ME is model error, f'_c is the concrete compressive strength, d is the effective depth, b is the beam width, $A_i(t)$ is the cross-sectional area of the i^{th} main reinforcing bar (A_{stnom}-$A_{pit}(t)$) and $f_{yi}(t)$ is the yield strength for the i^{th} reinforcing bar.

As these degradation processes (surface cracking and resistance degradation) include a large number of random variables and spatial random fields, Monte Carlo simulation is a powerful tool to solve this type of problem. With the appropriate corrosion models, the random field analysis can be used to predict the likelihood and extent of corrosion damage and the probability of structural collapse. A full description of random field modelling used in the present paper for surface cracking damage and the effect of pitting corrosion on structural safety is described elsewhere (Stewart and Mullard 2007, Stewart 2009).

4. RELIABILITY UPDATING BASED ON VISUAL INSPECTION

The extent of pitting corrosion of embedded multiple reinforcing bars is difficult to identify by non-destructive testing methods. The commonly used techniques to investigate the corrosion status of reinforcing bars are half-cell potential, concrete resistivity test and linear polarization methods. Each of these techniques provides some information related to the corrosion status, but each has its limitations. For example, the half-cell potential method only provides an assessment of the likelihood that there is active corrosion in the structure, but provides very little guidance about the corrosion rate. The linear polarization resistance technique can be used to estimate the rate of section loss of the bar based on Faraday's law for general (uniform) corrosion, but it is not suitable for chloride-induced pitting corrosion. Moreover, it has been reported that 3LP and Gecor corrosion rate field measurements differed from the actual corrosion rate by 20%-250% (Liu and Weyers 1998). Many other more advanced techniques, such as guided waves and embedded sensor, have been developed to detect the corrosion of hidden steels, but the associated high costs and need for advanced operating skills mean these techniques are not widely used in practice.

Corrosion-induced cover cracking is an early visible indication of corrosion in the concrete. Vu et al (2005) and Stewart and Mullard (2007) have correlated corrosion rate to corrosion-induced crack width, and so cover cracking is one indicator of corrosion loss and extent of structural resistance degradation, although there still remains uncertainty as to the extent and depth of pitting corrosion and the effect this has on temporal and spatial variability of structural capacity. As visual inspections are a common, and relatively inexpensive, non-destructive evaluation technique it is reasonable to attempt to infer as much useful information as possible from such inspections. Hence, known or inferred relationships between corrosion-induced crack width (corrosion damage), corrosion rate, and rebar cross-section loss will be used to update the structural reliability analysis and the variability of predictions can be reduced.

A routine visual inspection is a regularly scheduled inspection to determine the physical and functional condition of a structure and to identify any changes since previous inspections. If n inspections are conducted at times $t_1, t_2, \ldots, t_n$, where x_i% of surface with crack width $w(t_i)$ exceeding w_{lim} mm is observed at time t_i (i=1, 2, …, n) then the additional information available from visual inspection represented by H can be expressed as

$$H : \left[d_{crack}(t_1) = x_1\% \cap w(t_1) = w_{lim} \right] \cap \ldots\ldots \cap \left[d_{crack}(t_n) = x_n\% \cap w(t_n) = w_{lim} \right] \qquad (14)$$

Note that x_i% and $w(t_i)$ may equal to zero signifying the observation of no corrosion damage to the concrete cover. In the analysis it is assumed that corrosion damage information is revealed accurately during visual inspections, this may not always be the case and could result in an underestimation in failure probability.

Bayesian theorem relates the conditional and marginal probabilities of two random events which can often be interpreted as a conditional probability. It provides a rational method for incorporating existing information or judgments into predictions of future outcomes. The updated (posterior) proportion of a concrete surface with crack widths exceeding the limit width at time t for a single Monte Carlo simulation run is

$$d_{crack}^{upd}(t) = \frac{N\left[t > T_{i(j)} + T_{sp(j)} | H\right]}{m} \qquad (15)$$

where $N[t>T_{i(j)}+T_{sp(j)}|H]$ denotes the number of elements for which $t>T_{i(j)}+T_{sp(j)}$ conditional on the generated data matching the inspection information H.

Load and resistance are both stochastic processes, and for deteriorating structures the structural resistance reduces with time (see Figure 5). If K load events occur within the time interval (0, t) at times t_i (i = 1, 2,. . .,K) then the probability that a structure fails is:

$$p_f(t) = \Pr\left[G(t_1) < 0 \cup G(t_2) < 0 \cup ... \cup G(t_K) < 0\right] \quad \text{where} \quad t_1 < t_2 < ... < t_K \qquad (16)$$

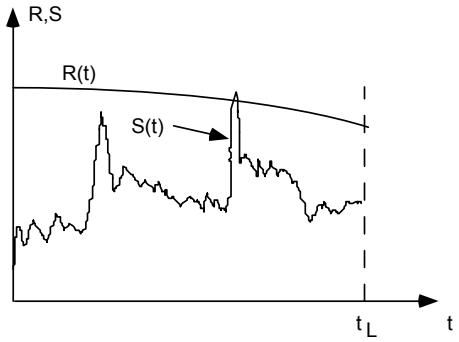

Figure 5 Resistance and Load Stochastic Processes

However, now assume that a condition assessment (in this case, visual inspection) is conducted at time t_{insp}, and that K load events occur within the time interval (0, t_{insp}) at times t_i (i = 1, 2,. . .,K) and that $t_K \leq t_{insp}$. After the condition assessment N loads events occur within the time interval (t_{insp},t). The result from the visual inspection is expressed as H. Service proven performance may be viewed as the structure surviving a series of service loads which act as 'proof 'loads (Stewart 1997). If the structure being inspected at time t_{insp} has survived t_{insp} years of loading up to this time, then the updated probability that a structure will fail in t years considering the condition assessment and t_{insp} years of service proven performance can be expressed as:

$$p_{f-insp}(t|t_{insp}) = \Pr\left[\{G(t_{n1}) < 0 \cup G(t_{n2}) < 0 \cup ... \cup G(t) < 0\} \middle| \{G(t_1) > 0 \cap G(t_2) > 0 \cap ... \cap G(t_K) > 0\}\right] \qquad (17)$$
$$\text{where} \quad t_K \leq t_{insp}, \; t_1 < t_2 < ... < t_K, \; t \geq t_{insp}, \; t > t_{n1} > t_{n2} > ... > t_{insp}$$

Monte-Carlo simulation techniques are used to solve Eqns. (16) and (17). As the concrete surface is discretised into m elements then m values of (T_i+T_{sp}) are obtained during each simulation run. If the damage condition of the surface generated by Monte-Carlo simulation matches the inspection data (H), the simulation result is recorded. Load effects and structural resistance are then calculated for each time step. Thus the recorded data reflects the current and future states of the structure considering the information obtained in the inspection. As the time steps proceed past the time of inspection, then the simulated time-dependent damage progression is used to infer updated cracking proportion given by Eqn. (15) and to assess if the ultimate strength limit state is exceeded. After many simulation runs, it is then possible to infer updated reliabilities.

5. NUMERICAL EXAMPLES

5.1 Structural Configuration

A simply supported RC beam measuring 0.4 m × 0.9 m × 10 m, which has survived 45 years of service, is analysed. The reinforcement is six 27 mm diameter bars with nominal yield strength f_y=410 MPa and the specified nominal strength of concrete is F_c'=34.5 MPa. The concrete cover for main reinforcing bars is 50 mm. The RC design to ACI-318 is $\phi R_{nom}=1.2G_n+1.6Q_n$ where G_n and Q_n are design dead and live loads (Q_n/G_n=1.0), and ϕ=0.9. Statistical parameters for stochastic loads are given by Stewart (2009) and statistical parameters for corrosion parameters, material properties, dimensions and model errors are shown in Table 2. The corrosion rate is modelled as time-variant and the cover cracking model used is based on Eqns. (3) and (4).

Table 2. Statistical Parameters for Corrosion, Material and Dimensional Variables

Parameter	Mean	COV	Distribution
C_o (surface Cl concentration)	3.05 kg/m^3	0.74	Lognormal
C_r (threshold Cl concentration)	2.4 kg/m^3	0.2	Normal
Model error T_{sp} (w_{lim}=1.0 mm)	1.05	0.20	Normal
Model error for flexure (ME)	1.01	0.046	Normal
Model error for D and i_{corr}	1.0	0.2	Normal
Cover	+1.6 mm	σ=11.1 mm	Normal
Concrete cylinder strength f'_{cyl}	F'_c+7.4 MPa	σ=6 MPa	Normal
k_w ($f'_c(28)=k_w f'_{cyl}$)	1.0	0.00	
Reinforcement yield strength (f_y)	465 MPa	0.098	Normal
Pitting factor (R)	8.62	0.14	Gumbel
Concrete tensile strength $f'_{ct}(t)$	$0.53(f'_c(t))^{0.5}$	0.13	Normal
Concrete elastic modulus $E'_c(t)$	$4600(f'_c(t))^{0.5}$	0.12	Normal

For simplification of illustration, only cracking induced by the corrosion of main reinforcing bars and the flexural limit state are considered herein. The beam is discretised into m=20 elements of length Δ=0.5 m (see Figure 3). A 1D random field is used to model the spatial variability of concrete cover, concrete compressive strength, surface chloride concentration and pitting factor of 20 elements. The correlation between every two elements is determined by the Gaussian correlation function which is commonly used in engineering applications. The scale of fluctuation for concrete cover, concrete compressive strength and surface chloride concentration used herein is 2.0 m.

5.2 Target Reliability

For structural safety assessment, a target reliability is necessary. The Danish Road Directorate guidelines for reliability assessment of existing bridges is used herein. As ductile mechanical behaviour of a RC beam is considered, the annual failure probability $P_{fA}=10^{-5}$ for collapse with warning is appropriate (DRD 2004). The cumulative target failure probability up to time t $P_{ft}(t)$, given it has survived t_{insp} years of service loading, is

$$P_{ft}(t) = 1 - \left(1 - P_{fA}\right)^{t - t_n} \qquad (18)$$

5.3 Inspection Scenarios

The inspection scenarios are assumed to investigate the influence of inspection findings on future failure probability predictions, see Table 3, where we assume that the inspection findings relate to corrosion damage observed over the entire beam and where crack width $w(t_1)=w(t_2)=1.0$ mm. For inspection scenarios A1 to A3, corrosion damage at time t_1=42 years equals to 0%, while the observed proportion of corrosion damage increases from 0% to 10% at time t_2=45 years. In all cases, the 'worst' corrosion damage is limited to 10%, as excessive corrosion damage, such as that in excess of 10%, would in most cases be promptly repaired or replaced in practice. Up to 200 million Monte-Carlo simulation runs matching the inspection findings are used to calculate the probabilities of structural collapse.

Table 3. Inspection Scenarios

Inspection Scenario	t_1 (years)	t_2 (years)	Inspection Result H	
			Severe Cracking at t_1 (x_1%)	Severe Cracking at t_2 (x_2%)
A1	42	45	0%	0%
A2	42	45	0%	5%
A3	42	45	0%	10%

5.4 Results

Figure 6 shows the mean percentage of the concrete surface that is severely cracked ($d_{crack}(t)$) for a RC bridge deck of 900 m^2 discretised into 3600 elements of size Δ=0.5 m (Stewart and Mullard 2007). This figure shows the probability distributions of extent of cracking at times of 40, 80 and 120 years. It is observed that the distributions of extent of cracking are non-Gaussian and there is significant likelihood of zero cracking, which reduces with time, and that the likelihood of significant cracking is low even after 120 years.

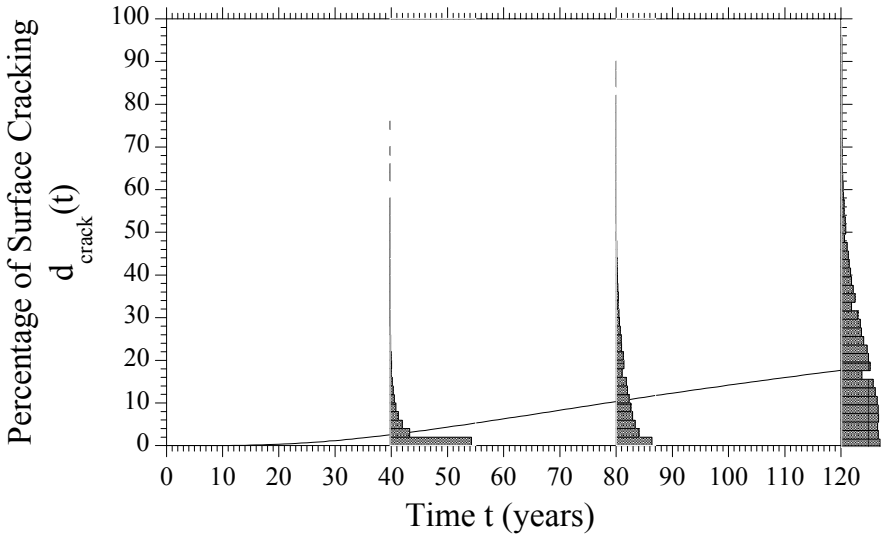

Figure 6 Mean Percentage of Surface Cracking and its Variability at t=40, 80 and 120 years, RC Bridge Deck and for w_{lim}=1.0 mm (Stewart and Mullard 2007).

Figure 7 shows the prior (no inspection) and updated mean proportion of severe cracking $d_{\text{crack}}(t)$ and $d^{\text{upd}}_{\text{crack}}(t)$, respectively, for inspection scenarios A1, A2 and A3. As expected, if no corrosion damage is observed (A1) then the updated mean of $d_{crack}(t)$ reduces, but the observation of damage (A2, A3) increases the updated mean of $d_{crack}(t)$. For more details on the effect of different inspection intervals and inspection times on proportions of severe cracking (corrosion damage) see Suo and Stewart (2009). If the criterion for a patch repair is 1% of the surface area exhibiting visual signs of concrete, then the first repair will occur when the extent of damage is observed to exceed X_{repair}=1% of total surface area. In this case, for inspection scenario A1 this would mean that expected time to first maintenance would be 54 years.

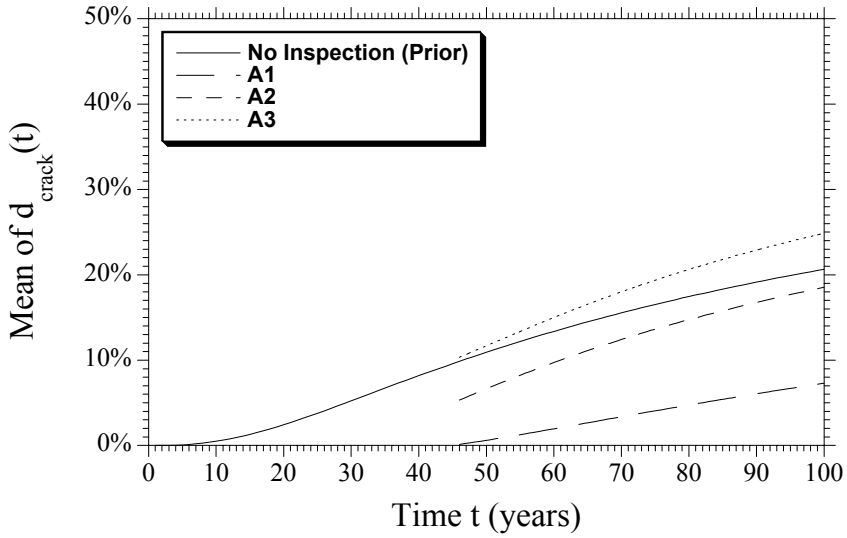

Figure 7 Prior and Updated Mean of Cracking Proportion.

The mean and standard deviation of flexural resistance of 20 elements conditional on the occurrence of inspection scenario A1, A2 and A3 are shown in Figures 8 and 9, respectively. The long term trends are as expected; namely, the higher the observed corrosion damage the larger is the reduction in mean structural resistance. Moreover, the standard deviation of structural resistance reduces with inspection findings, indicating the reduction in variability of updated predictions when inspection data are considered. Not surprisingly, at time of inspection the structure conditional on the occurrence of inspection scenario A3 has the lowest mean resistance.

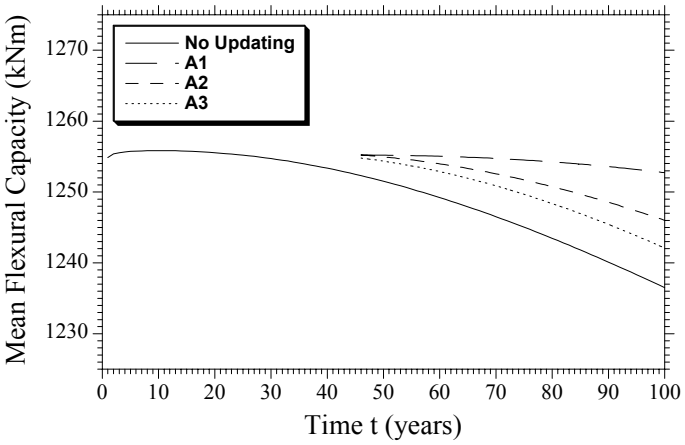

Figure 8 Prior (No Updating) and Updated Mean of Resistance.

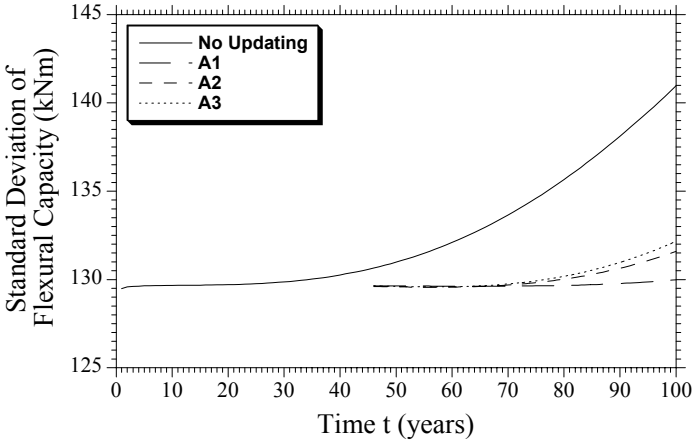

Figure 9 Prior and Updated Standard Deviation of Resistance.

The cumulative probabilities of failure $p_{f\text{-}insp}$ (t) are calculated from Eqn. (17) for structures conditional on inspection scenarios A1, A2 and A3 and service proven performance – see Figure 10. By means of comparison, the cumulative probability of failure considering no inspection data, but updated on service proven performance is also shown in Figure 10. A service proven reliability is also calculated assuming no deterioration over the life of the structure. The benefits of updating, in terms of increasing structural reliability, are immediately apparent from Figure 10. Figure 10 shows that updating based on service proven performance and inspection data results in probabilities of failure that are at least an order of magnitude lower than if updating is not considered.

It is easy to observe the obvious difference between structural reliabilities for inspection scenarios A1, A2 and A3 in Figure 10. The probability of failure is significantly decreased if the corrosion damage inspection information is used to update future predictions. If no corrosion damage is detected (inspection scenario A1) then the probability of failure is only slightly higher than the probability of failure based on no deterioration over the life of the structure. As more damage is detected the probability of failure increases. The failure probabilities are not significantly affected by the different inspection findings for the first 30 years after inspection. The reason that failure probability is not very sensitive to the change of corrosion damage findings, especially for inspection scenarios A2 and A3, is that corrosion damage is uniformly randomly distributed along the beam, while a higher proportion of governing ultimate limit states is at mid span. For an element at the end part of the beam with corrosion damage, because of the lower load effects, it is unlikely to be a critical vulnerable element, so the effects of corrosion damage on failure probability are diminished. The trends shown herein are similar if other inspection timings are used; for example, t_1=52 years and t_2=55 years.

Figure 10 also shows the cumulative target failure probability (P_{ft}), which as observed from Eqn. (18) will vary with time. Clearly, if no inspection data are used then the target failure probability is exceeded at the time of the second inspection (45 years). However, if no corrosion damage is observed (A1), and this new information is used to update estimates of structural reliability, then the target failure probability is not exceeded until 89 years – thus extending the predicted safe service life by 44 years. This is a significant extension of service life prediction. Even if some corrosion damage is detected during an inspection (A2, A3) then the predicted safe service life is still relatively high at 64 years. These examples illustrate the benefits of inspection updating on service life prediction.

Many more inspection scenarios can be considered. Those used herein simply help illustrate that the time-dependent structural performance and reliability can be updated with information after routine visual inspections and other condition assessment data. Note that these results deduced from inspection findings mainly depend on models used in the simulation, such as the correlation function and deterioration models and these models vary with service environment and inspection technique. Because visual inspection is a highly subjective non-destructive evaluation technique, the results of these inspections can be highly variable and are dependent on many factors. The updated and more accurate structural reliability

predictions containing latest condition assessment information can be used to improve asset management strategies such as inspection and maintenance schedules and costs, as well as more accurate service life prediction.

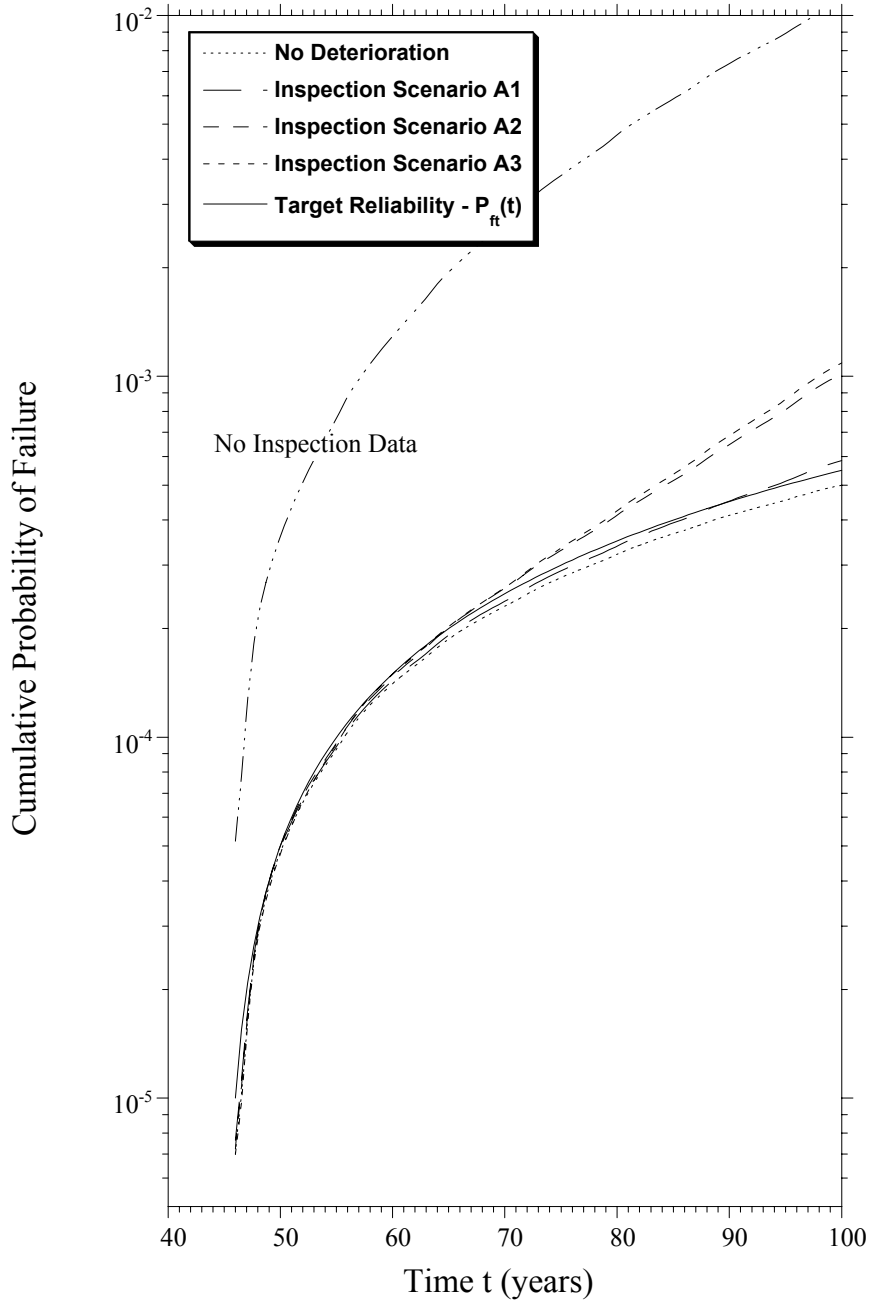

Figure 10 Probabilities of Failure for Inspection Scenarios A1-A3.

6. CONCLUSIONS

A procedure for adopting visual inspection findings to reliability safety assessment updating is presented in the paper. This process involves application of random field theory by which the structure is divided into many elements to better simulate its temporal and spatial deterioration characteristics. Chloride-induced corrosion and resulting concrete cover cracking can be modelled appropriately. The influence of visual inspection finding such as the timing, extent and location of corrosion damage (severe cover cracking) on structural reliability predictions is described. It was found that structural reliabilities have the potential to increase if service proven performance and inspection findings are used to update the structural reliability analysis. The role and benefits of inspection data in the safety assessment and service life prediction of exiting structures was illustrated for a typical RC beam subject to a marine environment.

7. ACKNOWLEDGEMENTS

The support of the Australian Research Council and the Cooperative Research Centre for Integrated Engineering Asset Management (ID207) are gratefully acknowledged. The assistance of Dr Qinghui Suo with computer programming and preparation of Figure 4 is also gratefully acknowledged.

8. REFERENCES

1. DRD, Reliability-Based Classification of the Load Carrying Capacity of Existing Bridges, Report 291, Danish Road Directorate, Denmark, 2004.

2. Du YG, Clark LA, Chan AHC. Residual capacity of corroded reinforcing bars. *Magazine of Concrete Research*, 57(3), 2005, 135-147

3. El Maaddawy TE, Soudki KA. Model for Prediction of Time from Corrosion Initiation to Corrosion Cracking. *Cement & Concrete Composites*, 29(3), 2007, 168-175.

4. Fazio R, Mirza MS, McCafferty E, Andrews RJ, Masheer PA and Long AE. In-situ Assessment of Corrosion Induced Damage of the Dickson Bridge Deck. In: *Proceedings of the 8th International Conference on Durability of Building Materials and Components*. Vancouver, Canada, 1999, 269-279.

5. Li Y, Vrouwenvelder T, Wijnants GH and Walraven J. Spatial variability of concrete deterioration and repair strategies. *Structural Concrete*, 5(3), 2004, 121-129.

6. Liu Y and Weyers RE. Modelling the Time-to-corrosion Cracking in Chloride Contaminated Reinforced Concrete Structures, *ACI Materials Journal*, 9(6), 1998, 675-681.

7. Mullard JA, Stewart MG, *Corrosion-Induced Cover Cracking of RC Structures: New Experimental Data and Predictive Models*, Research Report No. 275.01.2009, Centre for Infrastructure Performance and Reliability, The University of Newcastle, NSW, Australia, 2009.

8. Papadakis VG, Roumeliotis AP, Fardis MN, and Vagenas CG, , *Mathematical Modelling of Chloride Effect on Concrete Durability and Protection Measures*, Concrete Repair, Rehabilitation and Protection, R.K. Dhir and M.R. Jones (Eds.), 1996, pp. 165-174, E & FN Spon, London, UK.

9. Stewart MG, Time-Dependent Reliability of Existing RC Structures, *Journal of Structural Engineering*, ASCE, 123(7), 1997, 896-903.

10. Stewart MG, Spatial variability of pitting corrosion and its influence on structural fragility and reliability of RC beams in flexure. *Structural Safety* 26(4), 2004, 453-470

11. Stewart MG, Mullard JA. Spatial time-dependent reliability analysis of corrosion damage and the timing of first repair for RC structures. *Engineering Structures*, 29(7), 2007, 1457-1464.

12. Stewart MG, Al-Harthy A. Pitting corrosion and structural reliability of corroding RC structures: Experimental data and probabilistic analysis. *Reliability Engineering and System Safety*, 93(3), 2008, 373-392.

13. Stewart MG, Suo Q. Extent of spatially variable corrosion damage as an indicator of strength and time-dependent reliability of RC beams. *Engineering Structures*, 31(1), 2009, 198-207.

14. Stewart MG. Mechanical behaviour of pitting corrosion of flexural and shear reinforcement and its effect on structural reliability of corroding RC beams. *Structural Safety* 2009, 31(1), 19-30.

15. Suo Q, Stewart MG. Corrosion cracking prediction updating of deteriorating RC structures using inspection information. *Reliability Engineering and System Safety*, 94(8), 2009, 1340-1348.

16. Vanmarcke EH. *Random Field: analysis and synthesis*. Cambridge: The MIT Press; 1983.

17. Val DV, Stewart MG. Reliability assessment of ageing reinforced concrete structures – current situation and future challenges, *Structural Engineering International,* 19(2), 2009, 211-219.

18. Vu KAT, Stewart MG. Predicting the Likelihood and Extent of Reinforcement Concrete Corrosion-induced Cracking. *Journal of Structural Engineering*, 131(11), 2005, 1681-1689.

19. Vu KAT, Stewart MG, Mullard JA. Corrosion-induced Cracking: Experimental Data and Predictive Models. *ACI Structural Journal*, 102(5), 2005, 719-726.

20. Vu KAT, Stewart MG. Structural Reliability of Concrete Bridges Including Improved Chloride-induced Corrosion Models. *Structural Safety*, 22(4), 2000, 313-333.

9. AUTHOR DETAILS

Mark G. Stewart is a Professor of Civil Engineering and Director of the Centre for Infrastructure Performance and Reliability, School of Engineering, The University of Newcastle, Australia. His research interests include stochastic deterioration modelling, spatial structural and serviceability reliability analysis, probabilistic risk assessment, security risk assessment, and life-cycle cost and decision analysis. He has published over 250 technical papers on these and other topics.